Journal of Analytical Science and Technology

RESEARCH ARTICLE Open Access

A cationic quantum dot-based ratiometric fluorescent probe to visually detect berberine hydrochloride in human blood serums

Mingyang Liu[1], Xuejun Du[1], Ke Xu[1], Binwei Yan[1], Zaibi Fan[1], Zideng Gao[1*] and Xueqin Ren[1,2*]

Abstract

Berberine hydrochloride (BH) is an isoquinoline alkaloid normally used as drug to treat diseases. Compared with the traditional detection methods, the carbon quantum dots (CQDs) have better selectivity, high sensitivity, easy operation, and is inexpensive which could be widely utilized as fluorescent nanoprobes to detect various compounds quantificationally. And ratiometric fluorescent sensors conspicuously increase sensitivity and precision detection and improve quantification. In this work, we use water-soluble and fluorescent cationic carbon dots cetylpyridinium chloride monohydrate (CPC)-CQDs to connect with pinacyanol chloride (PC) and sodium tetraphenylborate (ST) as the ratiometric fluorescent probe to detect BH. The ratiometric fluorescent probe has high sensitivity towards alkaloids and metal ions, photochemical stability (60 min), and pH stability (from 6.0 to 8.0), with the detection range from 0 to 200 μM, and limit was as low as 57.35 nM. The accuracy of the method was verified by spiked recovery experiment in different human blood serums which were drawn from healthy adult volunteers to explore the practicability. The recoveries were in the range 94.34 to 105.48% with relative standard deviations (RSD) of 0.80 to 2.92%. In addition, we could observe that the fluorescence was gradually darkened, and the color turned yellow to realize the visual detection. It is expected that this work would open up a new strategy for detecting BH in the environment and human blood serums.

Keywords: Carbon quantum dots (CQDs), Fluorimetry, Berberine hydrochloride (BH), Ratiometric fluorescent probe, Visual detection

Introduction

Berberine hydrochloride (BH) is an isoquinoline alkaloid from the *Berberis* species. Because of the inhibitory effect on *Dysentery bacillus*, *Escherichia coli*, *Streptococcus aureus*, *Pneumococcus*, *Typhoid bacillus*, *and Amoeba*, the extensive anti-cancer and anti-inflammation effects have been widely used as drug to treat some diseases including diarrhea, dysentery, and stomatitis (X. W. Jiang et al., 2013). It also has certain curative effect on tuberculosis, scarlet fever, acute tonsillitis, and respiratory tract infection (J. S. Wang et al., 2020; Z. Wang et al., 2017). Up to now, the detection methods of BH include resonance Rayleigh scattering, ultraviolet spectrophotometry, chemiluminescence, fractional imprinting electrode, capillary electrophoresis, and fluorescence spectrometry (Biparva, Abedirad, Kazemi, & Shanehsaz, 2016; Liang, Kuang, Ma, Chen, & Long, 2016; S. P. Liu, Yang, Liu, Liu, & Shi, 2006). Most of detection methods require to use the expensive, sophisticated instrument and troublesome pretreatment procedures. Therefore, the establishment of a rapid and simple method for the detection of BH is of great significance. Fluorescence

* Correspondence: gzdsch@163.com; renxueqin@cau.edu.cn
[1]College of Resources and Environmental Sciences, China Agricultural University, Beijing 100193, China
Full list of author information is available at the end of the article

analysis has been widely used for pollutant analysis and detection in recent years because of its better selection, high sensitivity, uncomplicated instruments, low cost, and easy operation (Baker & Baker, 2010; Das, Bandyopadhyay, & Pramanik, 2018; Molaei, 2019). At the same time, as an environment-friendly optical probe, carbon quantum dots (CQDs) are widely used in the field of analysis and detection (Li, Kang, Liu, & Lee, 2012).

Fluorescent carbon nanoparticles or carbon quantum dots (CQDs) are a new class of carbon nanomaterials that have emerged recently, which have been identified as a new class of "zero-dimensional" nanomaterials (Li et al., 2012). On the account of CQDs have remarkable chemical and physical properties, such as, easy synthesis, high water solubility, stable fluorescence, low toxicity, and good biocompatibility, they have been widely applied in bioimaging, sensor, photocatalysis, drug delivery, and medical diagnosis (Feng, Ai, An, Yang, & Zhao, 2016; Guo, Zhang, Cao, & Leng, 2016; K. Jiang et al., 2015; Wu et al., 2016; Zhu et al., 2013). Since fluorescence sensing is usually aimed at small molecules, it is necessary to achieve highly selective quantitative determination of a given analyte. Although most of the fluorescent probes are absolute intensity-dependent signal readout, they may fail to accurately analyze the concentration of target substance because of the presence of various analyte-independent factors, such as instrument parameters, background light scattering, and the microenvironment around the probe molecule (Chen, Pradhan, Wang, Kim, & Yoon, 2012; Kim, Guo, Zhu, Yoon, & Tian, 2011; Kim, Ren, Kim, & Yoon, 2012; J. Shen, Shang, Chen, Wang, & Cai, 2017; Vaz et al., 2017). Ratiometric fluorescent sensors were proposed to overcome these problems and insure reliability. Ratiometric fluorescent sensors rely on the intensity of two or more emission bands and offer self-calibration for environmental interference which could conspicuously increase sensitivity and precision detection and improve quantification under conditions of quantitative analysis (Haidekker & Theodorakis, 2016; Kumar et al., 2016; J. T. Liu et al., 2009).

In this work, we designed a ratiometric fluorescent sensor to measure BH in the deionized water and human blood serums. Firstly, we synthesized cetylpyridinium chloride monohydrate (CPC)-CQDs according to a reported, rapid and eco-friendly method. Then, CPC-CQDs conjugated with pinacyanol chloride (PC) and sodium tetraphenylborate (ST) to build the ratiometric fluorescent probe. We studied the fluorescence response of the sensing sensor to BH, with the detection range from 0 to 200 μM, and limit was as low as 57.35 nM. In addition, we measured the high resistance of the probe for metal ions and alkaloid reagents, photostability (60 min), and pH stability (from 6.0 to 8.0). The accuracy of the method was verified by spiked recovery experiment in different human blood serums which were taken from healthy adult volunteers from Peking University Third Hospital to explore the practicability. In addition, we could observe that the fluorescence was gradually darkened, and the color turned yellow to realize the visual detection. All in all, this ratiometric fluorescent probe could be used to detect BH visually, sensitively, and precisely.

Materials and methods

Chemicals

Pinacyanol chloride (PC), sodium tetraphenylborate (ST), cetylpyridinium chloride monohydrate (CPC), and all detected objects (berberine hydrochloride (BH), omeprazole (OPZ), D-tetrandrine, reserpine, quinidine, sulfamethazine (SM2), sulfapyridine) were purchased from Shanghai Aladdin, Ltd. (Shanghai, China). All metal salts (AgCl, $BaCl_2{\cdot}2H_2O$, $FeCl_2$, $FeCl_3$, $CdCl_2{\cdot}2½H_2O$, $ZnSO_4$, $MgCl_2{\cdot}6H_2O$, $CuSO_4$, $CaCl_2$, $CoCl_2{\cdot}6H_2O$) were supplied from Sinopharm Chemical Reagent Co., Ltd. (Beijing, China). Deionized water and tap water were obtained from the laboratory in China Agricultural University (Beijing, China).

Instrument

The morphologies of CPC-CQDs were characterized by transmission electron microscope (TEM) and high-resolution transmission electron microscope (HRTEM) (STEM; FEI Tecnai G2 F30, 300 kV). Fourier transform infrared (FTIR) spectra were recorded on a Nicolet NEXUS-470 Spectrometer (Madison, USA), using the KBr pellet method. X-ray photoelectron spectroscopy (XPS) from Thermo Escalab 250Xi (USA) was acquired and processed by the advanced advantage data system in order to investigate the chemical structures. Fluorescence spectra were recorded on an F-7000 fluorescence spectrophotometer (Hitachi, Tokyo, Japan). Ultraviolet −visible (UV-Vis) spectra were recorded on a WTF UV-2102PC UV-Vis spectrophotometer (UNICO Shanghai Instrument Co., Ltd., China).

Preparation of CPC-CQDs and the fluorescent probe

The CPC-CQDs were prepared according to the previously reported method (Gao et al., 2019). CPC-CQDs were carbon quantum dots with CPC as the carbon source. The setting of reaction conditions (including NaOH concentration, response time, and temperature) would affect the properties of CQDs. By comparison, the CQDs were synthesized via a simple method: 400 μL of 1 M NaOH was added into 10 mL CPC solution (50 mM), followed by ultrasonic treatment at room temperature for 12 h. To end the synthetic reaction, adding HCl into the solution to adjust pH to 7.0. Then, the solution was extracted by dichloromethane solution to get the upper and dialyzed for 48 h with dialysis bags in

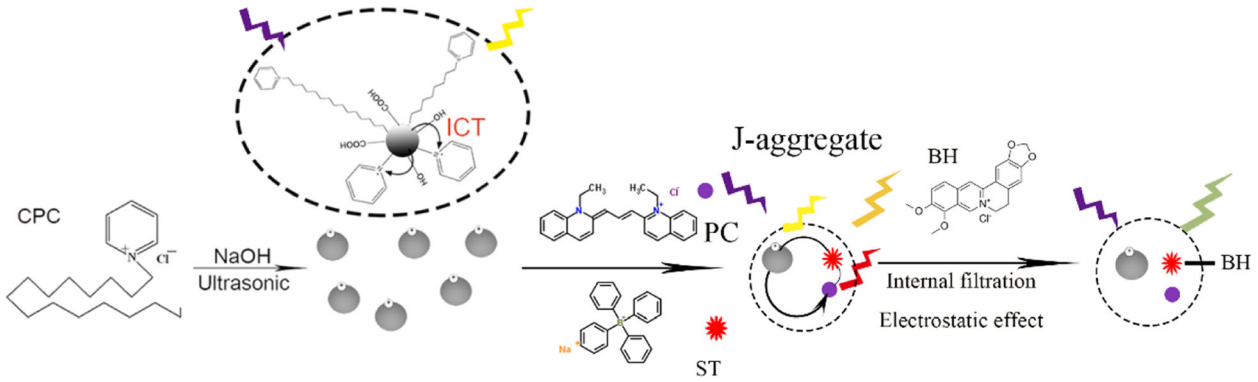

Scheme 1 Preparation process of CPC-CQDs, the sensing probe, and the proposed sensing mechanism

deionized water to remove interference substances. After vacuum freeze drying, we could obtain the CPC-CQDs powder. Then, we prepared the sensing probe: adding 0.05 mg CPC-CQDs, 1 μL of 1 mM PC solution, and 25 μL of 1 mM tetraphenylborate solution into 1 mL sample.

Quantum yields

Q_Y of the CPC-CQDs was calculated as:

$$\Phi_X = \Phi_s \left(\frac{A \rightleftarrows_s}{A_x}\right)\left(\frac{I_x}{I_{st}}\right)\left(\frac{\eta_x \rightleftarrows^2}{\eta_s{}^2}\right) \quad (1)$$

where Φs is the Q_Y of the standard, A is the optical density, I is absorbance at the excitation wavelength (370 nm), η is the refractive index of the solvent (both are 1.33), x subscript denotes unknown, and s is the standard (rhodamine B).

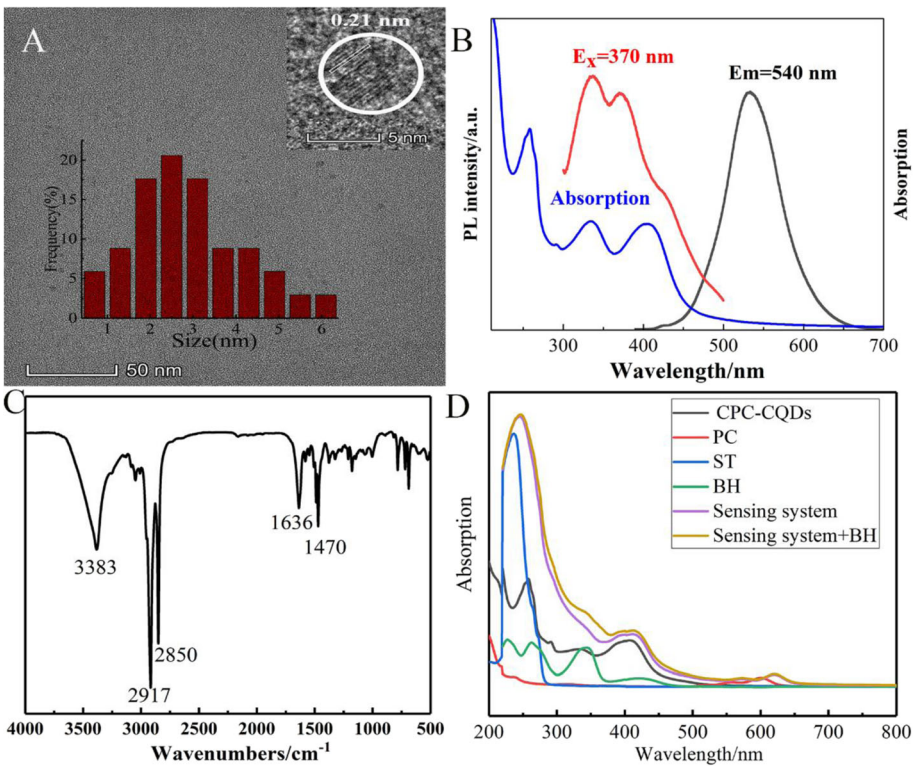

Fig. 1 **a** TEM images of CPC-CQDs (inset: HRTEM image of CPC-CQDs; background: particle size distribution of CPC-CQDs). **b** Absorption (blue), excitation spectra (red), and emission spectra (black) of CPC-CQDs. **c** FTIR spectra of CPC-CQDs. **d** Absorption of the materials and mixture

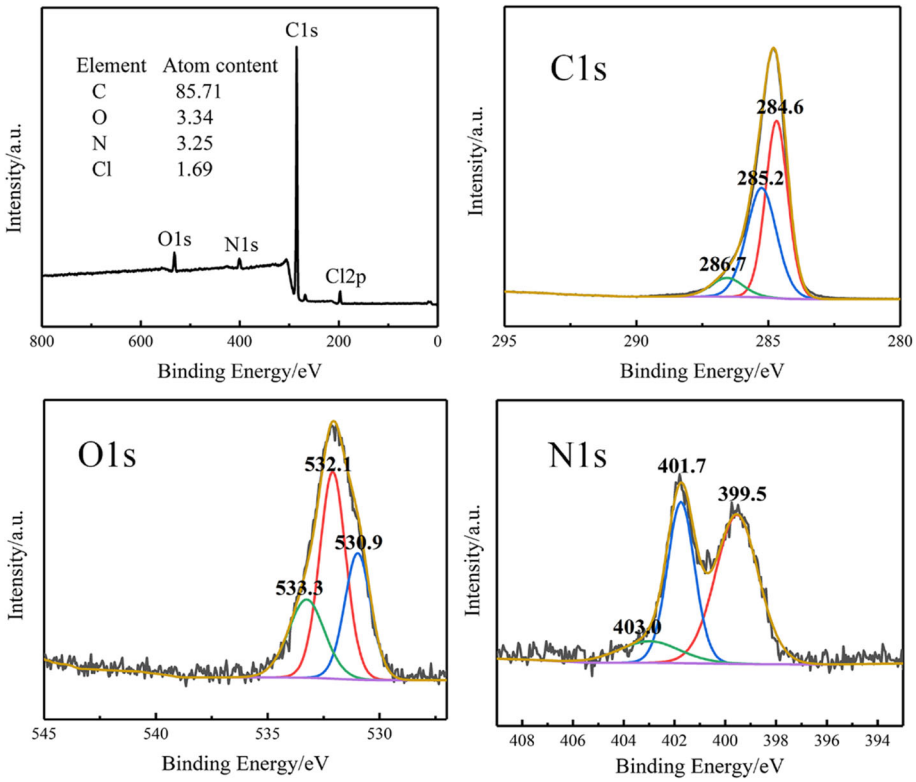

Fig. 2 X-ray photoelectron spectroscopy (XPS) spectra of CPC-CQDs (**a**) and C1s, O1s, and N1s of CPC-CQDs (**b**, **c**, and **d**) respectively

Assay procedures

The detection of BH was performed at room temperature in deionized water. The change in fluorescence intensity was recorded at 370 nm after adding different concentrations of BH (from 0 to 200 μM) under well-mixing conditions. Then, the same concentration (50 μM) of metal ions and alkaloid reagents was added to study the selectivity and anti-interference of the CPC-CQDs. In addition, we investigated the photostability and pH stability by recoding the fluorescence intensity change every 10 min under 1 h and pH from 5.0 to 9.0.

Preparation of real samples

To investigate the detection of BH by the detecting system in real samples, we prepared different human blood serums. Human blood serums were taken from healthy adult volunteers from Peking University Third Hospital. The blood samples were pretreated to eliminate any protein interference and to improve the recovery, adding 3 mL portion of trichloroacetic acid (quality fraction 15%) to 1 mL serum to destroy the activity of proteins in the serum and to precipitate them from the solution. The mixture was centrifuged at 10,000 rpm for 10 min after vigorous shaking for 15 min. The supernatant was obtained and modulated to pH 7.0 utilizing NaOH solution. The treated serum samples were diluted 50 times using deionized water.

Results and discussion

Characterizations of CPC-CQDs and ratiometric fluorescent probe

As shown in Scheme 1, to obtain CPC-CQDs, we adopted a simple and efficient "bottom-up" method (Feng et al., 2016). CPC-CQDs were carbon quantum dots with CPC as the carbon source because the CPC-CQDs had positively charged surfaces, so it could as the electron donor group (EDG). While quaternary ammonium group could as the electron withdrawing group (EWG), formed a "push-pull" electron conjugate system (D-π-A), which showed yellow fluorescence emission (Zheng et al., 2015). We study the morphology, optical, and structure of the CPC-CQDs through TEM image, HRTEM image, XPS, UV–vis absorption, FTIR, and fluorescence spectra.

The morphology and particle size of CPC-CQDs were characterized by transmission electron microscopy (TEM) and high resolution transmission electron microscopy (HRTEM). As shown in Fig. 1a, the small black dots in the picture were carbon dots; we could observe that the synthesized CPC-CQDs were uniformly distributed without aggregation. The particle size of the

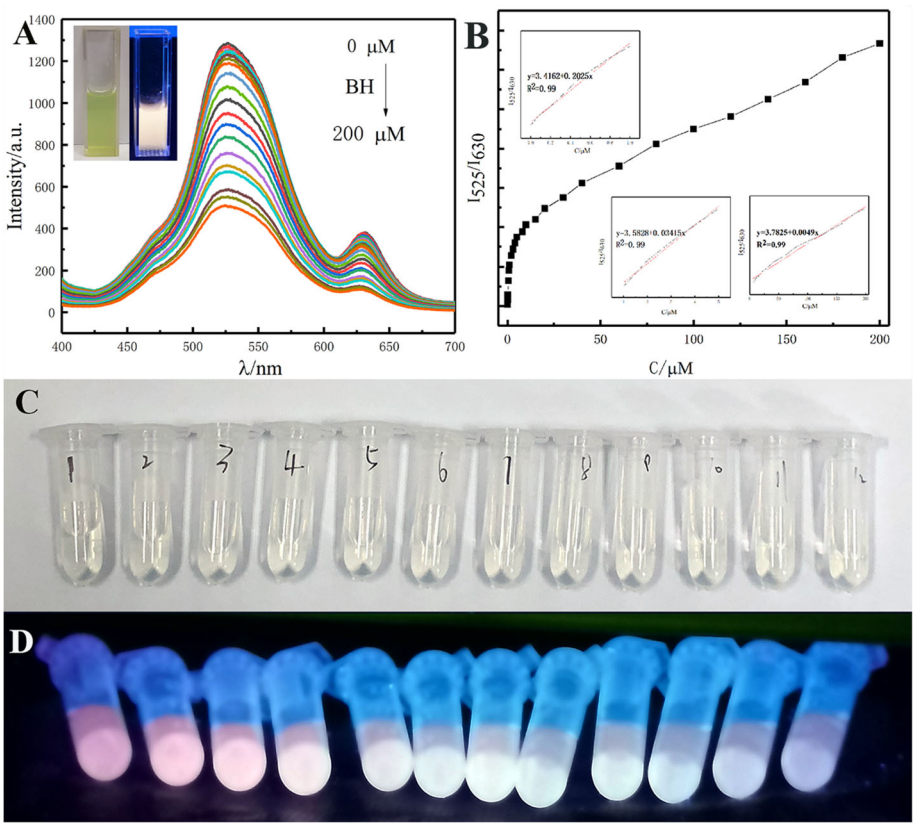

Fig. 3 **a** Fluorescence emission spectra of ratiometric fluorescent probe respond to different concentrations of BH (from 0 to 200 μM) (insets showed the fluorescence color change under a 365-nm UV lamp in the presence of 50 μM BH (right) and blank (left)), **b** fluorescence intensity of ratiometric fluorescent probe changed in the range of 0–200 μM BH (insert: linear relationship between the fluorescent ratio of I_{525}/I_{630} and the BH concentrations). The color change of the sensing sensor responds to different BH concentrations (0, 0.001, 0.005, 0.01, 0.05, 0.1, 0.5, 1, 2, 3, 4, 5 μM) **c** under daylight and **d** a 365-nm UV lamp

synthesized CPC-CQDs was found mainly distributed from 0.78 to 6.10 nm, with an average particle size of 3.20 nm, on analyzing 100 individual particles. HRTEM image demonstrated a lattice spacing of 0.21 nm corresponding to graphene (1100) plane (Zheng, Ananthanarayanan, Luo, & Chen, 2015).

From Fig. 1b, we could research the optical properties of CPC-CQDs. The fluorescence emission peak of CPC-CQDs was at 540 nm, and the fluorescence excitation peak was at 340 nm and 370 nm;. in this work, we used the 370 nm as the E_X wavelength because the absorption peak of BH at 340 nm overlapped resulting in internal filtration. In addition, when we irradiated the carbon quantum dot solution with UV lamp at 365 nm, the solution was bright orange (Fig. 3a inset). Furthermore, the quantum yield (Q_Y) of the prepared CPC-CQDs was determined to be 22.30% (Guan, Huang, Qian, & Yu, 2017).

As shown in the Fig. 1c, we could speculate the functional groups on the surface of CPC-CQDs by FTIR experiments. The characteristic absorption peaks at 3383 cm^{-1} ascribed to O–H/N–H stretching bond, at 2917 cm^{-1} and 2850 cm^{-1} for the stretching vibration of C–H, CH_3 and CH_2 moieties, and the peaks at 1636 cm^{-1} and 1470 cm^{-1} were assigned to C=C and C=N in pyridine, respectively. The series of bands from 1636 to 1470 cm^{-1} were ascribed to a CH_2 stretching vibration deformation (Hu et al., 2014; Prasannan & Imae, 2013).

Figure 1d showed the UV absorption spectra of the materials and the mixture. The two peaks at 334 and 400 nm of CPC-CQDs refer to the π–π* transitions of aromatic sp^2 domains and n–π* transitions. We speculated the fluorescence quenching mechanism from the UV absorption spectra and the fluorescence spectra. It could be seen that BH had absorption peaks at 227, 263, 343, and 420 nm. The fluorescence emission peak and the fluorescence excitation peak of CPC-CQDs were at 540 nm, 340 nm, and 370 nm, respectively. The excitation and emission spectra overlapped with the absorption spectra of BH, so the fluorescence quenching may be caused by the internal filtration between them (Xu et al., 2020). What's more, the fluorescence static quenching caused by electrostatic effect was another reason for fluorescence quenching. The second peak of fluorescence quenching at 630 nm quenched faster than

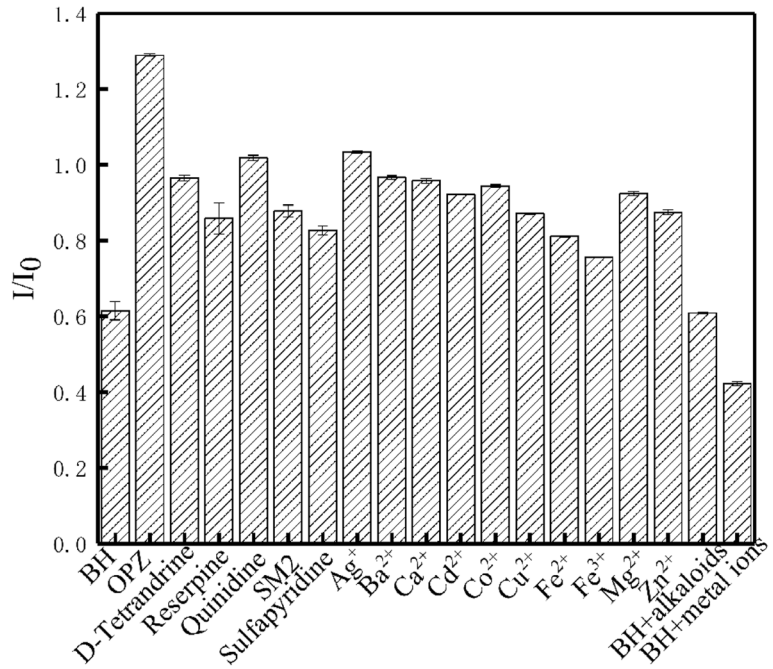

Fig. 4 Selectivity of the CPC-CQDs sensors in the presence of 50 μM various alkaloids and metal ions

the fluorescence peak at 525 nm because CPC-CQDs and PC were positive electrical conductivity, and sodium tetraphenylborate was negative electrical conductivity (Gao et al., 2019; Lee, Kim, & Sessler, 2015). The sensing probe could connect with BH through electrostatic effect resulting in fluorescence quenching. In conclusion, fluorescence quenching mechanism of BH on the ratiometric fluorescent probe is synergistic effect of internal filtration and static quenching induced by electrostatic action.

XPS measurement could further investigate the surface functional groups and elemental states of CPC-CQDs as shown in the Fig. 2. The XPS survey (Fig. 2a) showed that CPC-CQDs mainly contain carbon (C1s), oxygen (O1s), and nitrogen (N1s), and their composition contents were 85.71%, 3.34%, and 3.25% respectively. Among them, the C1s spectrum of CPC-CQDs (Fig. 2b) showed three peaks at 284.6 eV, 285.2 eV, and 286.7 eV, respectively, indicating that the carbon belongs to three different chemical environments, corresponding to C–C/C=C, C–O/C–N, and C=O/O–C=O groups, respectively (Huang et al., 2014; J. Wang, Wang, & Chen, 2012). Then, we analyzed the O1s spectra, as shown in Fig. 2c; the O1s spectra show three peaks at 530.9 eV, 532.1 eV, and 533.3 eV, which referred to C–O, C=O, and C–OH/C–O–C groups (Wohlgemuth, White, Willinger, Titirici, & Antonietti, 2012). In the high-resolution N1s spectra (Fig. 2d), the three peaks at 399.5, 401.7, and 403.0 eV could be attributed to C–N–C, N^+–4C, and N–H groups (Lu et al., 2012). Together with the analysis of FTIR, these analytical results indicated the pyridinium rings and various of aliphatic carbon on the surface of CPC-CQDs.

Then, adding PC (positive charged) and ST (electrical charged) to build a ratiometric fluorescent probe to detect BH. Because of the mechanism of J-aggregate, the sensing system showed orange fluorescence emission in visual (Deshmukh et al., 2020; C. A. Shen & Wurthner, 2020; Sun et al., 2020; Zhang et al., 2020). The ratiometric fluorescent probe showed two fluorescence emission peaks at 525 nm and 630 nm.

Fluorescence response of ratiometric fluorescent probe to BH

Figure 3a displayed the fluorescence intensity of the ratiometric fluorescent probe decreased at different extent at 525 nm and 630 nm with an increase in the BH concentration from 0 to 200 μM. And we could observed that the fluorescence color changes from orange to yellow. As shown in Fig. 3b, it could be seen that the fluorescent intensity ratio (I_{525}/I_{630}) increased with the addition of BH to the solution. And I_{525}/I_{630} (Fig. 3b insert) exhibited good linearity with the concentration of BH ranging from 0 to 1 μM, 1 to 5 μM, and 5 to 200 μM. The linear regression equation is $I_{525}/I_{630} = 0.2025C + 3.4162$ ($R^2 = 0.99$) from 0 to 1 μM; $I_{525}/I_{630} = 0.3415C + 3.5828$ ($R^2 = 0.99$) from 1 to 5 μM; and $I_{525}/I_{630} = 0.0049C + 3.7825$ ($R^2 = 0.99$) from 5 to 200 μM, in which, I refers to the fluorescence intensities and C refers to the concentration of BH. The detection limit was recorded to

be 57.35 nM from 3 σ/m (Wu, Su, Wang, Wong, & Zhu, 2017). As shown in Fig. 3c and d, we could see the fluorescence change of the solution with the increase of the concentration of BH from 0 to 5 μM. The fluorescence intensity decreased with the addition of BH, and the fluorescence color gradually turned yellow and dark.

Selectivity and stability of the sensing system

For BH sensing in a complex environment, we tested the selectivity and anti-interference performance of this sensor during some potential interferences including detected objects (OPZ, D-tetrandrine, reserpine, quinidine, SM2, sulfapyridine), metal ions (Ag^{+}, Ba^{2+}, Ca^{2+}, Cd^{2+}, Co^{2+}, Cu^{2+}, Fe^{2+}, Fe^{3+}, Mg^{2+}, Zn^{2+}), and the mixture under the same conditions (50 μM). I/I_0 referred to the ratio of I_{525}/I_{630} in the presence and absence of these interferential ions. As shown in Fig. 4, other ions displayed weak or even negligible effects on their fluorescence intensities compared with BH. The fluorescence intensity was almost the same as that of single BH, with a slight decrease in that of the metal mixture, mainly due to the quenching of iron and the BH. It is proved that this probe has good selectivity.

To study the stability of CPC-CQDs and the sensing probe, the fluorescence intensity of CPC-CQDs and the sensing probe were measured under the conditions of varying pH and long-term illumination. We investigated the photostability and pH stability of CPC-CQDs and the sensing probe. Figure 5a and c showed fluorescence intensity of CPC-CQDs and the sensing probe as a function of pH. From Fig. 5a, we could speculate that CPC-CQDs had no obvious change when the pH increased from 5.0 to 9.0. But for the fluorescent probe, because pH would affect the ionization of water, affecting the J-aggregate light emission between CPC-CQDs, QB, and ST, resulting in a decrease in the fluorescence intensity of the two peaks at 525 nm and 630 nm. As shown as Fig. 5c, the fluorescence intensity of the two peaks decreased to a similar degree, which indicated the sensing probe had no obvious change when the pH was from 6.0 to 8.0. Figure 5b and d showed that the fluorescence intensity of CPC-CQDs and the sensing probe was as almost unchanged under 60 min continuous UV irradiation indicating that it had good bleaching resistance, and the stability time range was relatively wide. Excellent stability provided possible applications for the sensing probe in complex system.

Application in real samples

To explore the practicability of the sensing probe for the detection, the accuracy of the method was verified by spiked recovery experiment in different human blood serums taken from healthy adult volunteers from Peking

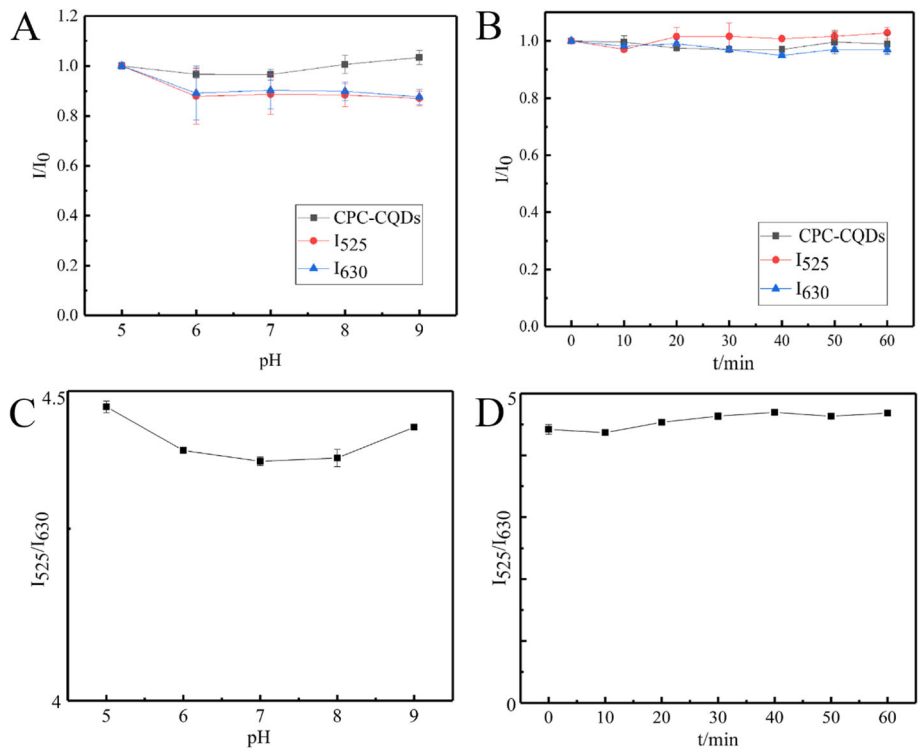

Fig. 5 The pH stability (**a**, **c**) and photostability under continuous UV irradiation (**b**, **d**) of CPC-CQDs and the fluorescent probe

Table 1 Detection of berberine hydrochloride in blood samples

Sample	Add (μM)	Found (μM)	Recovery (%, $n = 5$)	RSD (%)
Sample 1	40	42.19	105.48	2.92
	50	51.47	102.93	3.27
	60	56.60	94.34	1.15
Sample 2	30	29.75	99.15	1.96
	60	60.17	100.28	1.57
	70	73.21	104.59	0.99
Sample 3	10	10.01	100.06	0.97
	15	14.66	97.72	1.32
	40	40.70	101.75	0.80

University Third Hospital. And then, we pretreated the blood samples to eliminate protein interference. As shown in Table 1, the recoveries of blood sample 1 were in the range 94.34 to 105.48% with relative standard deviations (RSD) of 1.15 to 2.92%; the recoveries of blood sample 2 were in the range 99.15 to 104.59% with relative standard deviations (RSD) of 0.99 to 1.96%; the recoveries of blood sample 3 were in the range 97.72 to 101.75% with relative standard deviations (RSD) of 0.80 to 1.32%. The result indicated that the sensing system could be an efficient probe to detect BH in human blood serum samples. As shown in Table 2, the CPC-CQDs in this work performed well compared with the analytical performance of some relevant works for BH detection.

Conclusion

We built a ratiometric fluorescent sensor which could conspicuously increase sensitivity and precision detection and improve quantification to realize visual detection of BH in the environment. We build a cationic carbon quantum fluorescent probe based on CPC-CQDs, PC, and ST. We used the mechanism of J-aggregate; the sensing system showed orange fluorescence emission in visual. The fluorescence-quenching mechanism of BH on the ratiometric fluorescent probe is synergistic effect of internal filtration and static quenching induced by electrostatic action. The sensing system has high sensitivity and selectivity towards alkaloids and metal ions, photochemical stability (60 min), and pH stability (from 6.0 to 8.0), with the detection range from 0 to 200 μM, and limit was as low as 57.35 nM. The accuracy of the method was verified by spiked recovery experiment in different human blood serums to explore the practicability. The CPC-CQDs-based fluorescence detection system possesses promising potential in the environmental and bioassay applications.

Table 2 Comparison of several typical methods for BH detection

Sensor system	LOD/μM	Linear range/μM	Ref.
HPTS	1.24	2.0–50	Guo et al. (2019)
PTMA	0.27	0.3–13.0	Gao et al. (2020)
SiO_2NPs	0.002	0.005–0.13	Liu et al. (2018)
BNOB	0.20	0.4–282	Liu et al. (1998)
F-AuNCs	0.075	1–100	Wen et al. (2018)
PDPA	0.75	0.75–750	Huang et al. (2002)
Ag NPs	0.013	0.05–0.4	Ling et al. (2008)
CPC	0.057	0–200	This work

Abbreviations

BH: Berberine hydrochloride; CQDs: Carbon quantum dots; PC: Pinacyanol chloride; ST: Sodium tetraphenylborate; CPC: Cetylpyridinium chloride monohydrate; TEM: Transmission electron microscope; HRTEM: High-resolution transmission electron microscope; FTIR: Fourier transform infrared; XPS: X-ray photoelectron spectroscopy; UV-Vis: Ultraviolet–visible spectra

Acknowledgements

Not applicable.

Authors' contributions

This study was designed by Mingyang Liu. The experimental work was performed by Xuejun Du and Ke Xu. Mingyang Liu drafted the manuscript; Binwei Yan and Zaibi Fan analyzed the data. Zideng Gao and Xueqin Ren reviewed and edited the manuscript. All authors read and approved the final manuscript.

Funding

This work was financially supported by the Key Technologies Research and Development Program of China (2017YFD0200706, 2016YFC0501205, and 2016YFC0501208) and the National Natural Science Foundation of China (21775163).

Availability of data and materials

All the experiments were carried out at College of Resources and Environment Sciences, China Agricultural University, Beijing. Analytical data (TEM, HRTEM, FTIR, and XPS) were measured at the institution of Zhong Ke Bai Ce, Beijing. All the data are available from the corresponding author (Dr. Xueqin Ren) of this manuscript.

Competing interests

The authors declare no competing interests.

Author details

[1]College of Resources and Environmental Sciences, China Agricultural University, Beijing 100193, China. [2]Beijing Key Laboratory of Farmland Soil Pollution Prevention and Remediation, China Agricultural University, Beijing 100193, China.

Received: 25 September 2020 Accepted: 1 February 2021
Published online: 24 February 2021

References

Baker SN, Baker GA. Luminescent carbon nanodots: emergent nanolights. Angew Chem Int Ed Engl. 2010;49(38):6726–44.
Biparva P, Abedirad SM, Kazemi SY, Shanehsaz M. Chemiluminescence recognition of berberine triggered by biomimetically synthesized silver nanoparticles. Sensors and Actuators B: Chemical. 2016;234:278–85.
Chen X, Pradhan T, Wang F, Kim JS, Yoon J. Fluorescent chemosensors based on spiroring-opening of xanthenes and related derivatives. Chem Rev. 2012; 112(3):1910–56.
Das R, Bandyopadhyay R, Pramanik P. Carbon quantum dots from natural resource: a review. Materials Today Chemistry. 2018;8:96–109.
Deshmukh AP, Bailey AD, Forte LS, Shen X, Geue N, Sletten EM, Caram JR. Thermodynamic control over molecular aggregate assembly enables tunable excitonic properties across the visible and near-infrared. J Phys Chem Lett. 2020;11:8026–33.

Feng T, Ai X, An G, Yang P, Zhao Y. Charge-convertible carbon dots for imaging-guided drug delivery with enhanced in vivo cancer therapeutic efficiency. ACS Nano. 2016;10(4):4410–20.
Gao Z, Wang S, Xu Z, Liu J, Huang Y, Hu S, Ren X. Synthesis of novel cationic carbon dots and application to quantitative detection of K+ in human serum samples. New J Chem. 2019;43(46):17937–40.
Gao X, Guo M, Liu M, Zhang L, Yao Z. A Fluorometric and Colorimetric Approach for the Rapid Detection of Berberine Hydrochloride Based on an Anionic Polythiophene Derivative. Luminescence. 2020.
Guan YF, Huang BC, Qian C, Yu HQ. Quantification of humic substances in natural water using nitrogen-doped carbon dots. Environ Sci Technol. 2017; 51(24):14092–9.
Guo Y, Zhang L, Cao F, Leng Y. Thermal treatment of hair for the synthesis of sustainable carbon quantum dots and the applications for sensing Hg(2). Sci Rep. 2016;6:35795.
Guo M, Li W, Sun Y, Xu H, Fan Y, Ma L, Huang, K, Yao Z. Rapid and visual detection of berberine hydrochloride based on a water-soluble pyrene derivative. Luminescence. 2019;34(6):558–62.
Haidekker MA, Theodorakis EA. Ratiometric mechanosensitive fluorescent dyes: design and applications. J Mater Chem C Mater. 2016;4(14):2707–18.
Hu Q, Paau M, Choi M, Zhang Y, Gong X, Zhang L, Liu Y, Yao J. Better understanding of carbon nanoparticles via high-performance liquid chromatography-fluorescence detection and mass spectrometry. Electrophoresis. 2014;35:2454.
Huang J, Zhong Z, Rong M, Zhou X, Chen X, Zhang M. An easy approach of preparing strongly luminescent carbon dots and their polymer based composites for enhancing solar cell efficiency. Carbon. 2014;70:190–8.
Jiang K, Sun S, Zhang L, Lu Y, Wu A, Cai C, Lin H. Red, green, and blue luminescence by carbon dots: full-color emission tuning and multicolor cellular imaging. Angew Chem Int Ed Engl. 2015;54(18):5360–3.
Jiang XW, Zhang Y, Zhu YL, Zhang H, Lu K, Li FF, Peng HY. Effects of berberine gelatin on recurrent aphthous stomatitis: a randomized, placebo-controlled, double-blind trial in a Chinese cohort. Oral Surg Oral Med Oral Pathol Oral Radiol. 2013;115(2):212–7.
Huang HM, Wang KM, Yang RH, Yang XH, Huang SS, Xiao D, Feng F. A sensitive optode membrane for berberine using conjugated polymer as sensing material. Anal Sci. 2002;18(10):1111–5.
Kim HN, Guo Z, Zhu W, Yoon J, Tian H. Recent progress on polymer-based fluorescent and colorimetric chemosensors. Chem Soc Rev. 2011;40(1):79–93.
Kim HN, Ren WX, Kim JS, Yoon J. Fluorescent and colorimetric sensors for detection of lead, cadmium, and mercury ions. Chem Soc Rev. 2012;41(8): 3210–44.
Kumar S, Verma T, Mukherjee R, Ariese F, Somasundaram K, Umapathy S. Raman and infra-red microspectroscopy: towards quantitative evaluation for clinical research by ratiometric analysis. Chem Soc Rev. 2016;45(7):1879–900.
Lee MH, Kim JS, Sessler JL. Small molecule-based ratiometric fluorescence probes for cations, anions and biomolecules. Chem Soc Rev. 2015;44(13):4185–91.
Li H, Kang Z, Liu Y, Lee S-T. Carbon nanodots: synthesis, properties and applications. J Mater Chem. 2012;22(46):24230.
Liang S, Kuang Y, Ma F, Chen S, Long Y. A sensitive spectrofluorometric method for detection of berberine hydrochloride using Ag nanoclusters directed by natural fish sperm DNA. Biosens Bioelectron. 2016;85:758–63.
Liu JT, Helms MW, Mandella MJ, Crawford JM, Kino GS, Contag CH. Quantifying cell-surface biomarker expression in thick tissues with ratiometric three-dimensional microscopy. Biophys J. 2009;96(6):2405–14.
Liu SP, Yang Z, Liu ZF, Liu JT, Shi Y. Resonance Rayleigh scattering study on the interaction of gold nanoparticles with berberine hydrochloride and its analytical application. Anal Chim Acta. 2006;572(2):283–9.
Liu Q, Xie Z, Liu T, Fan J. Determination of berberine hydrochloride using a fluorimetric method with silica nanoparticles as a probe. RSC Advances. 2018; 8(11):6075–82.
Liu WH, Wang Y, Tang JH, Shen GL, Yu RQ. An optical fiber sensor for berberine based on immobilized 1,4-bis(naphth[2,1-d]oxazole-2-yl)benzene in a new copolymer. Talanta. 1998;46(4):679–88.
Ling J, Sang Y, Huang CZ. Visual colorimetric detection of berberine hydrochloride with silver nanoparticles. J Pharm Biomed Anal. 2008;47(4-5): 860–4.
Lu W, Qin X, Liu S, Chang G, Zhang Y, Luo Y, Asiri AM, Al-Youbi AO, Sun X. Economical, green synthesis of fluorescent carbon nanoparticles and their use as probes for sensitive and selective detection of mercury(II) ions. Anal Chem. 2012;84(12):5351–7.
Molaei MJ. A review on nanostructured carbon quantum dots and their applications in biotechnology, sensors and chemiluminescene. Talanta. 2019; 196:456–78.
Prasannan A, Imae T. One-pot synthesis of fluorescent carbon dots from orange waste peels. Industrial Eng Chem Res. 2013;52:15673–8.
Shen CA, Wurthner F. NIR-emitting squaraine J-aggregate nanosheets. Chem Commun (Camb). 2020;56(68):9878–81.
Shen J, Shang S, Chen X, Wang D, Cai Y. Highly fluorescent N, S-co-doped carbon dots and their potential applications as antioxidants and sensitive probes for Cr (VI) detection. Sensors Actuators B: Chemical. 2017;248:92–100.
Sun B, Xu X, Zhou G, Tao L, Xinran W, Chen Z, Xu JB. Observation of strong J-aggregate light emission in monolayer molecular crystal on hexagonal boron nitride. J Phys Chem A. 2020;124(37):7340–5.
Vaz R, Bettini J, Júnior JGF, Lima EDS, Botero WG, Santos JCC, Schiavon MA. High luminescent carbon dots as an eco-friendly fluorescence sensor for Cr(VI) determination in water and soil samples. J Photochem Photobiol A: Chemistry. 2017;346:502–11.
Wang J, Wang CF, Chen S. Amphiphilic egg-derived carbon dots: rapid plasma fabrication, pyrolysis process, and multicolor printing patterns. Angew Chem Int Ed Engl. 2012;51(37):9297–301.
Wang JS, Sakthivel R, Anbazhagan R, Krishnamoorthi R, Kubendhiran S, Lai JY, Tsai HC, Chen SM. Electroactive polypyrrole-molybdenum disulfide nanocomposite for ultrasensitive detection of berberine in rat plasma. Anal Chim Acta. 2020;1125:210–9.
Wang Z, Wang YS, Chang ZM, Li L, Zhang Y, Lu MM, Zheng X, Li M, Shao D, Li J, Chen L, Dong WF. Berberine-loaded Janus nanocarriers for magnetic field-enhanced therapy against hepatocellular carcinoma. Chem Biol Drug Des. 2017;89(3):464–9.
Wen AL, Peng XX, Zhang PP, Long YF, Gong HM, Xie QR, Yue M, Chen S. Spectrofluorometric determination of berberine using a novel Au nanocluster with large Stokes shift. Anal Bioanal Chem. 2018;410(25):6489–95.
Wohlgemuth S-A, White RJ, Willinger M-G, Titirici M-M, Antonietti M. A one-pot hydrothermal synthesis of sulfur and nitrogen doped carbon aerogels with enhanced electrocatalytic activity in the oxygen reduction reaction. Green Chem. 2012;14(5):1515.
Wu F, Su H, Wang K, Wong WK, Zhu X. Facile synthesis of N-rich carbon quantum dots from porphyrins as efficient probes for bioimaging and biosensing in living cells. Int J Nanomedicine. 2017;12:7375–91.
Wu F, Su H, Zhu X, Wang K, Zhang Z, Wong WK. Near-infrared emissive lanthanide hybridized carbon quantum dots for bioimaging applications. J Mater Chem B. 2016;4(38):6366–72.
Xu Z, Wang Z, Liu M, Yan B, Ren X, Gao Z. Machine learning assisted dual-channel carbon quantum dots-based fluorescence sensor array for detection of tetracyclines. Spectrochim Acta A Mol Biomol Spectrosc. 2020;232:118147.
Zhang Y, Liu P, Pan H, Dai H, Ren XK, Chen Z. Alignment of supramolecular J-aggregates based on uracil-functionalized BODIPY dye for polarized photoluminescence. Chem Commun (Camb). 2020;56:12069.
Zheng XT, Ananthanarayanan A, Luo KQ, Chen P. Glowing graphene quantum dots and carbon dots: properties, syntheses and biological applications. Small. 2015;11(14):1620–36.
Zhu S, Meng Q, Wang L, Zhang J, Song Y, Jin H, Zhang K, Sun H, Wang H, Yang B. Highly photoluminescent carbon dots for multicolor patterning, sensors and bioimaging. Angew Chem Int Ed Engl. 2013;52(14):3953–7.

Publisher's Note